CURTISS-WRIGHT
IMR TEST LABS

131 Woodsedge Drive
Lansing, NY 14882
T: 607.533.7000 | F: 607.533.9210
www.imrtest.com

ANALYSIS OF PUMP SHAFT COUPLINGS

IMR Report Number 201000000

SUMMARY

Fracture of both AB12345C jack shafts and 98765 modular gear shaft occurred due to fatigue cracks initiating at areas of excessive fretting wear. Fatigue cracks initiated at the engagement points on the male tangs of each component, propagating through approximately half of the tang thickness, at which point final overload occurred.

Metallurgical evaluation of each component reveals significant amounts of retained austenite, as well as intergranular oxidation in the carburized case. Both conditions are known to adversely affect the fatigue life and wear resistance of carburized parts. The total case depth and observed case hardness of the samples was typical of that observed with a carburized low alloy steel.

Minimizing the amount of retained austenite (lowering carburizing temperature, cryogenic treatment prior to tempering, modification of quench rate) and intergranular oxidation (maintaining proper carburizing atmosphere and dew point) will help to curtail the observed fractures.

Evaluation of the comparison jack shaft reveals a powder metal component with significant porosity and a mixed microstructure. These conditions would tend to decrease performance and life expectancy. However, geometry and dimensional variation between this component and the AB12345C jack shafts may provide better load distribution thus extending service life.

Both AB12345C jack shafts **meet** the chemical requirements of UNS-G-86200 for an AISI 8620 nickel-chromium-molybdenum alloy steel. The 98765 modular gear shaft is **similar** in chemical composition to UNS-G-86200 for an AISI 8620 nickel-chromium-molybdenum alloy steel with the exception of the carbon concentration being high. UNS-G-86200 is given as a reference. No domestic match could be found for the comparison jack shaft. It is most consistent with an ASTM B426 grade 4 copper-steel or FX-2008 P/M material with lower than specified copper concentration.

February 23, 2010

Pete Greene
ABC Company
123 Main Street
Lansing, NY 14882

PO Number
P00001-AB

Date Received
January 1, 2010

Drawing #
98765, 20101234567, AB12345C

ACCREDITED 1140.01 + 1140.02

Accredited Nadcap Materials Testing Laboratory

Prepared by	Reviewed by
Tim Mueller	George Wildridge
Lead Metallurgist	Director of Metallurgy

MATERIAL RECEIVED

Multiple fractured shaft coupling components (jack shafts), a fractured modular drive shaft, an un-broken pump shaft, and the test stand interface were received. The drive shafts and both couplings had failed at their male tangs during use. Additionally, a jack shaft, which purportedly exhibits greater durability, was received for comparison. Typical components are shown, as received, in Figure 1.

METHODS

The following methods were used in this analysis:

1) Dimensional Analysis
2) Visual Examination
3) Fracture Surface Examination
4) Microstructure
5) Hardness
6) Chemistry

RESULTS

DIMENSIONAL ANALYSIS

Prior to examination, the male and female contact regions from the geared shafts, jack shafts, and test stand interface were measured for width. Results are provided in the following table.

Part	Male Tang[1] (Inches)	Female Slot[1] (Inches)
Test Stand Interface	---	0.2603
AB12345C Jack Shaft Incomplete Fracture	0.2403	0.3225
AB12345C Jack Shaft Complete Fracture	0.2383	0.3228
Comparison Jack Shaft	0.2983	0.3215
98765 Shaft	0.2372	---
20101234567 Shaft	0.3090	---

[1]Average of three readings.

It should be noted significant clearance (<0.02”) is present between mating portions of the components. This would tend to concentrate loads at the ends of the tang, causing higher than expected loading in these regions. It was also noted that the jack shaft provided for comparison has a significantly longer and wider tang, which may help to distribute loads more uniformly (see Figure 2).

VISUAL EXAMINATION

Examination of the fractured components reveals significant wear at the corners of the male tang on both the jack shafts and geared shaft. Red/black discoloration was observed on the worn surfaces. Similar features were noted on the test stand interface; however, the wear and associated discoloration was less pronounced. See Figures 3 – 5. Wear and discoloration of this type are consistent with fretting, which occurs due to oscillation or rubbing between mating surfaces.

After opening the cracked jack shaft to expose the fracture surface, the samples were cleaned for further evaluation. All three samples showed similar fractographic features: A smooth, reflective region of crack initiation, with beach marks (macroscopic fracture features indicative of fatigue) propagating to the approximate mid-point of the sample, followed by a region of final overload. Initiation was typically between the midpoint and top surface of the worn area in the male tang. See Figures 6 – 8.

FRACTURE SURFACE EXAMINATION

The fracture surfaces, as well as discoloration observed in the worn regions, were examined using a scanning electron microscope with energy dispersive spectroscopy (SEM/EDS). This instrument is equipped with a light element detector capable of detecting carbon and elements with greater atomic numbers (i.e., cannot detect hydrogen, helium, lithium, and beryllium).

EDS analysis of worn areas reveals the discoloration consists primarily of carbon, oxygen and iron. Silicon, aluminum, sulfur and chromium are present in lesser amounts (Figure 9). The carbon and metallic elements are all present in the substrate material to some extent, with the remaining carbon due to the lubricating grease used on the components. The oxygen is most likely present as an oxide (iron oxide). The presence of significant amounts oxygen in the worn regions supports wear by a fretting mechanism.

The fracture features observed on both jack shafts, as well as the 98765 gear shaft, were similar. Each component contains a region at the fracture origin with no distinct fractographic features, rubbed smooth by post fracture damage. Examination of regions with macroscopically visible beach marks reveals crack propagation occurred via cyclic loading (fatigue). Final overload regions for each component are comprised of dimpled rupture in the more ductile core, with intergranular separation in the case hardened regions. Figure 10 shows a macroscopic view of the fracture surface, with annotations providing approximate locations of the higher magnification images shown in Figures 11 – 16.

MICROSTRUCTURE

Longitudinal sections of the broken jack shafts, the comparison jack shaft, and the 98765 gear shaft were removed, mounted in epoxy, metallographically prepared to a 1 µm final polish, and examined in the as-polished and etched (2% nital) condition.

Examination in the as-polished condition reveals the extent of material loss at the engagement points of the jack shafts and 98765 gear shaft. Wear depth was much greater on the 98765 gear shaft than either of the two jack shafts. See Figure 17. Secondary cracking, beneath the primary fracture, was observed on the jack shaft with fractures on both sides of the male tang (Figure 18). No secondary cracks were observed on the 98765 gear shaft or cracked jack shaft. Intergranular oxidation was noted at the surface of each sample, ranging in depth from 2 to 10 µm (Figures 19 – 21). Intergranular oxidation is known to adversely affect fatigue resistance.

The microstructure of each component was similar, consisting of martensite and retained austenite in the case hardened region, with martensite and some ferrite in the core (Figures 22 – 24). Retained austenite percentage was estimated visually based on photographs within the Metals Handbook, Atlas of Microstructures, 8th Edition, Volume 7. Percent retained austenite for both jack shafts is estimated to be 30 – 35%, while the 98765 gear shaft contained 20 – 25%*. Significant amounts of retained austenite are considered detrimental, as austenite is soft – causing accelerated wear, and can be transformed to un-tempered martensite (which is brittle and can contribute to crack initiation) under load.

Total case depth was measured on the jack shafts and 98765 gear shaft in un-worn areas. Results are provided in the following table.

Sample	Total Case Depth[1] (inches)	Specification (inches)
98765 Gear Shaft	0.019	0.015 – 0.025
Jack Shaft – complete fracture	0.018	0.015 minimum
Jack Shaft – incomplete fracture	0.019	0.015 minimum

[1]Average of five readings.
Method: SAE J423-98

Examination of the jack shaft provided for comparison reveals a pressed and sintered powder metal material, with pores present at prior particle boundaries. Porosity was uniformly distributed throughout the sample cross section, and was measured at 13% via image analysis. Free copper was present throughout the microstructure, located primarily at prior particle boundaries. See Figure 25. No evidence of intergranular oxidation was observed.

Etching of the comparison jack shaft reveals a mixed microstructure consisting of martensite, bainite and fine pearlite throughout the cross section (Figures 26 and 27). The mixed microstructure indicates heat removal from the austenitizing temperature was not rapid enough to cause complete transformation to martensite. No retained austenite was observed.

*Note that for accurate determination of percent retained austenite, x-ray diffraction should be utilized.

MICROHARDNESS

Microhardness testing was conducted in the case and core of each sample using the samples prepared for microstructural evaluation after the etched surface was removed. A Knoop indenter and 500g load were utilized for the wrought materials (fractured jack shafts and 98765 gear shaft); a 100g load was used for the comparison jack shafts. Hardness of the carburized jack shaft and 98765 gear shaft was consistent with that typically observed in a case-hardened and tempered low alloy steel. Particle hardness readings of comparison jack shaft varied widely, as expected based on the observed microstructure. Results are provided in the following table.

Sample	Location	HK[1]	HRC[2]	Specification
98765 shaft	0.002″ below surface	649	56	56 – 58 HRC
	core	414	41	32 – 45 HRC
Jack Shaft - fractured	0.002″ below surface	656	56	---
	core	420	42	42 – 45 HRC
Jack Shaft – incomplete fracture	0.002″ below surface	656	56	---
	core	419	41*	42 – 45 HRC
Comparison Jack Shaft	0.002″ below surface	647	56	---
	core	460	45	---

*Fails to meet specification.
[1]Average of three readings.
[2]Converted from HK values.
Methods: ASTM E 384-09 and ASTM E 140-07

While core hardness of the jack shaft exhibiting incomplete fracture was lower than specified, this is not considered to be contributory to the fracture.

CHEMISTRY

Element	AB12345C Jack Shaft Complete Fracture	AB12345C Jack Shaft Incomplete Fracture	98765 Gear Shaft	UNS-G-86200
C[1]	0.19	0.20	0.27*	0.18 - 0.23
Cr	0.49	0.48	0.50	0.40 - 0.60
Mn	0.73	0.74	0.80	0.70 - 0.90
Mo	0.18	0.18	0.17	0.15 - 0.25
Ni	0.45	0.44	0.45	0.40 - 0.70
P	0.008	<0.005	<0.005	0.035 Maximum
S[1]	0.020	0.020	0.030	0.040 Maximum
Si	0.22	0.22	0.19	0.15 - 0.35
Al	<0.01	<0.01	0.02	---
Cu	0.21	0.21	0.13	---

[1]Determined by combustion-infrared absorbance.
*Fails to meet UNS-G-86200.
Results in weight percent unless otherwise indicated.
Method(s): CAP-017K (ICP-AES) and ASTM E 1019-08

Element	Comparison Jack Shaft
Al	<0.01
C[1]	0.71
Cr	0.06
Cu	14.84
Mn	0.12
Mo	<0.01
Ni	0.07
P	<0.005
S[1]	0.005
Si	0.02

[1]Determined by combustion-infrared absorbance.
Results in weight percent unless otherwise indicated.
Method(s): CAP-017K (ICP-AES) and ASTM E 1019-08

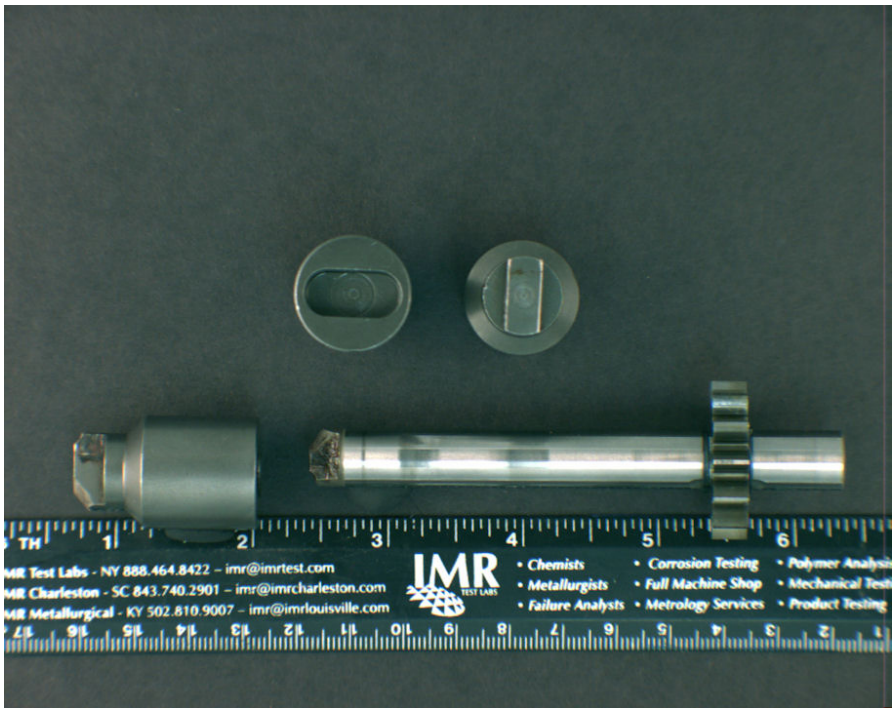

Figure 1: Components, as received.

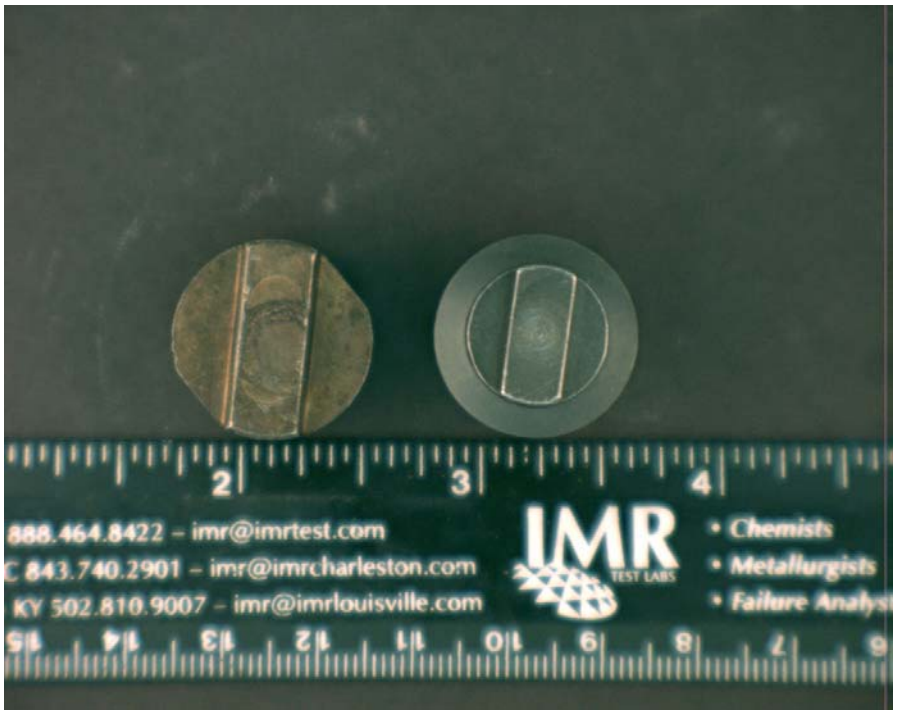

Figure 2: Image showing the difference in engagement length between the two jack shafts.

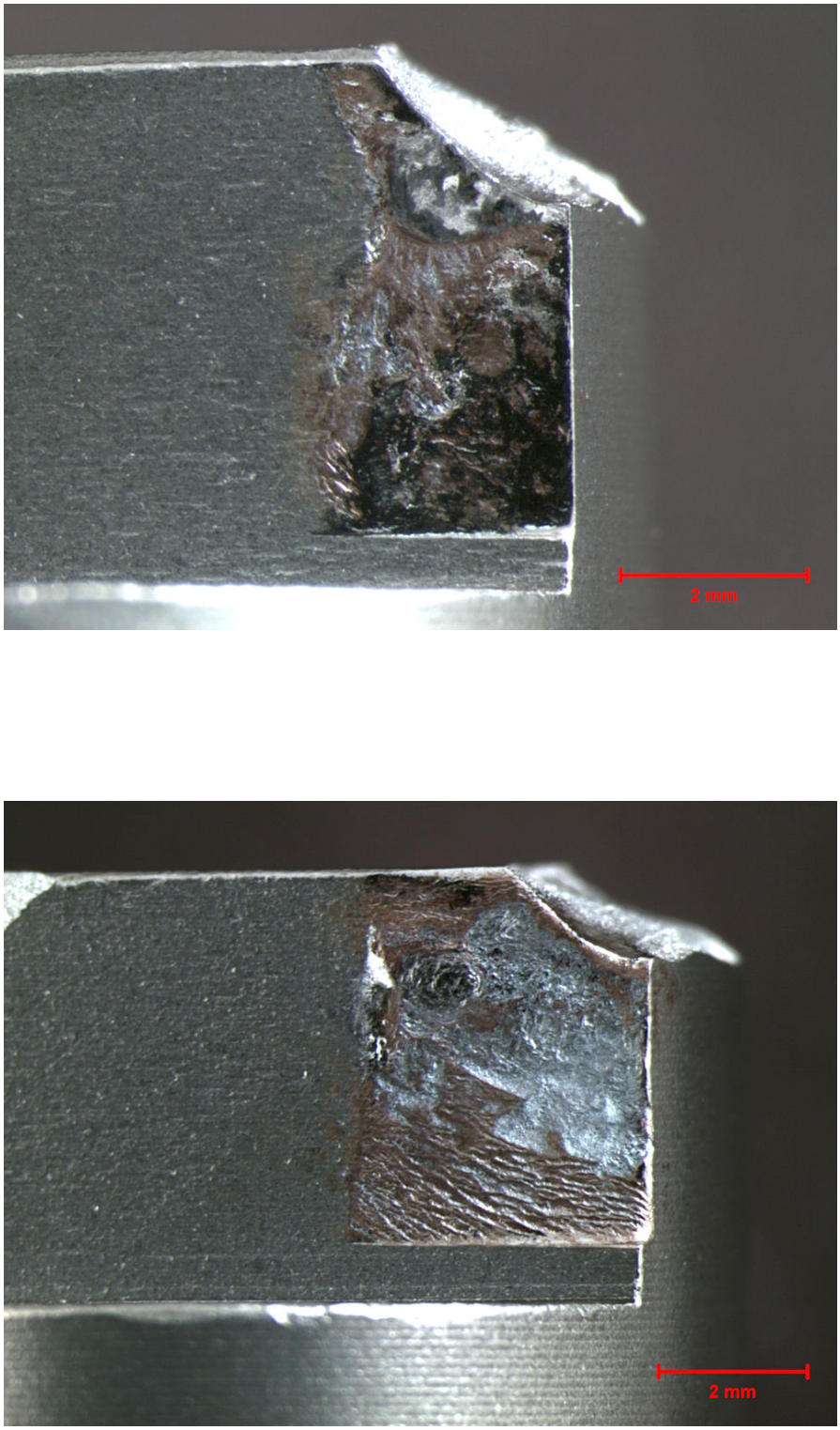

Figure 3: Wear pattern and associated reddish-black oxidation products were observed at the engagement points of cracked (top image – crack has been opened in this view) and fractured jack shafts.

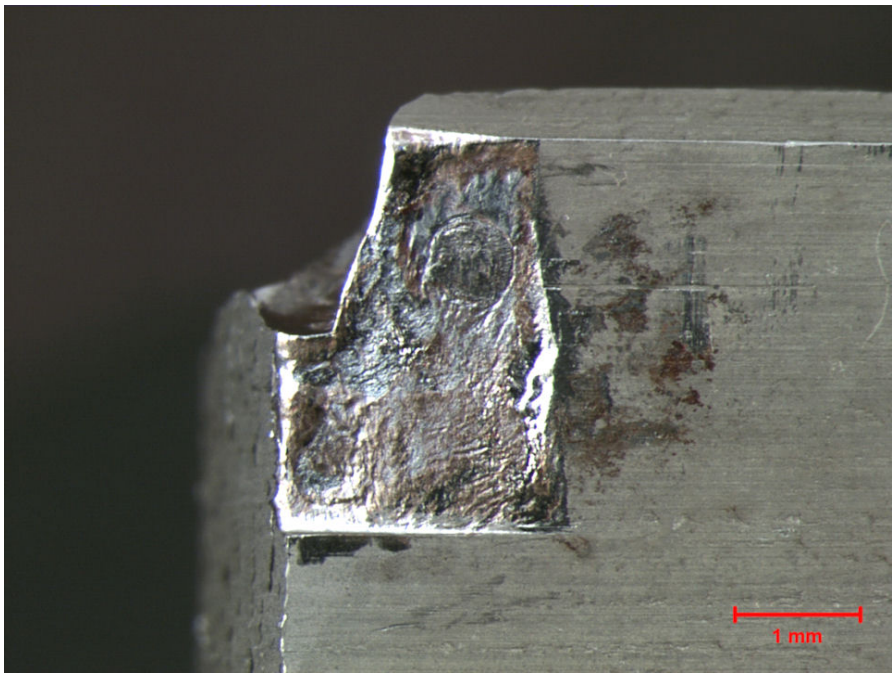

Figure 4: A similar wear pattern was observed at the 98765 shaft engagement points.

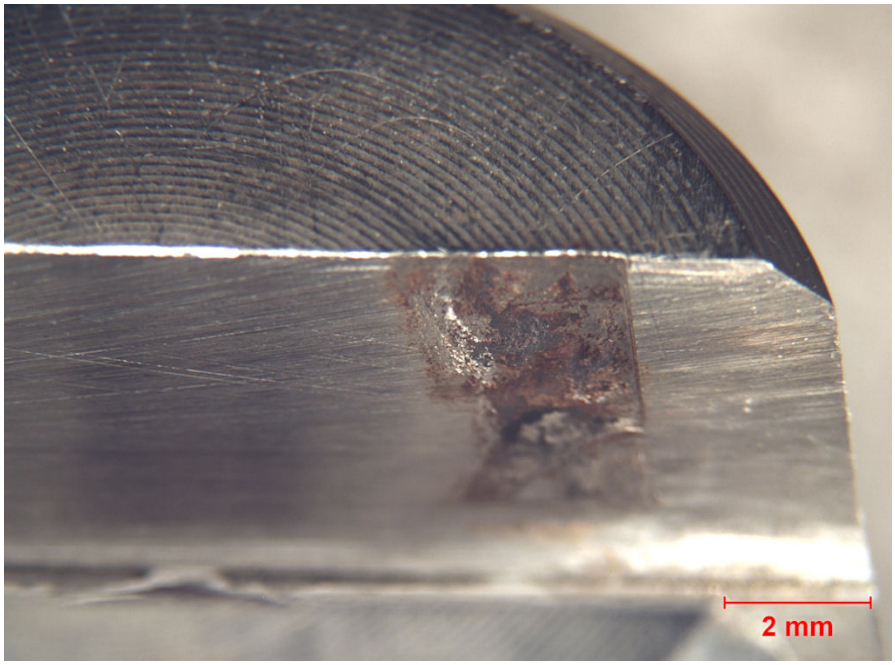

Figure 5: Wear observed on the test-stand fixture was not as extensive as that observed on the couplings.

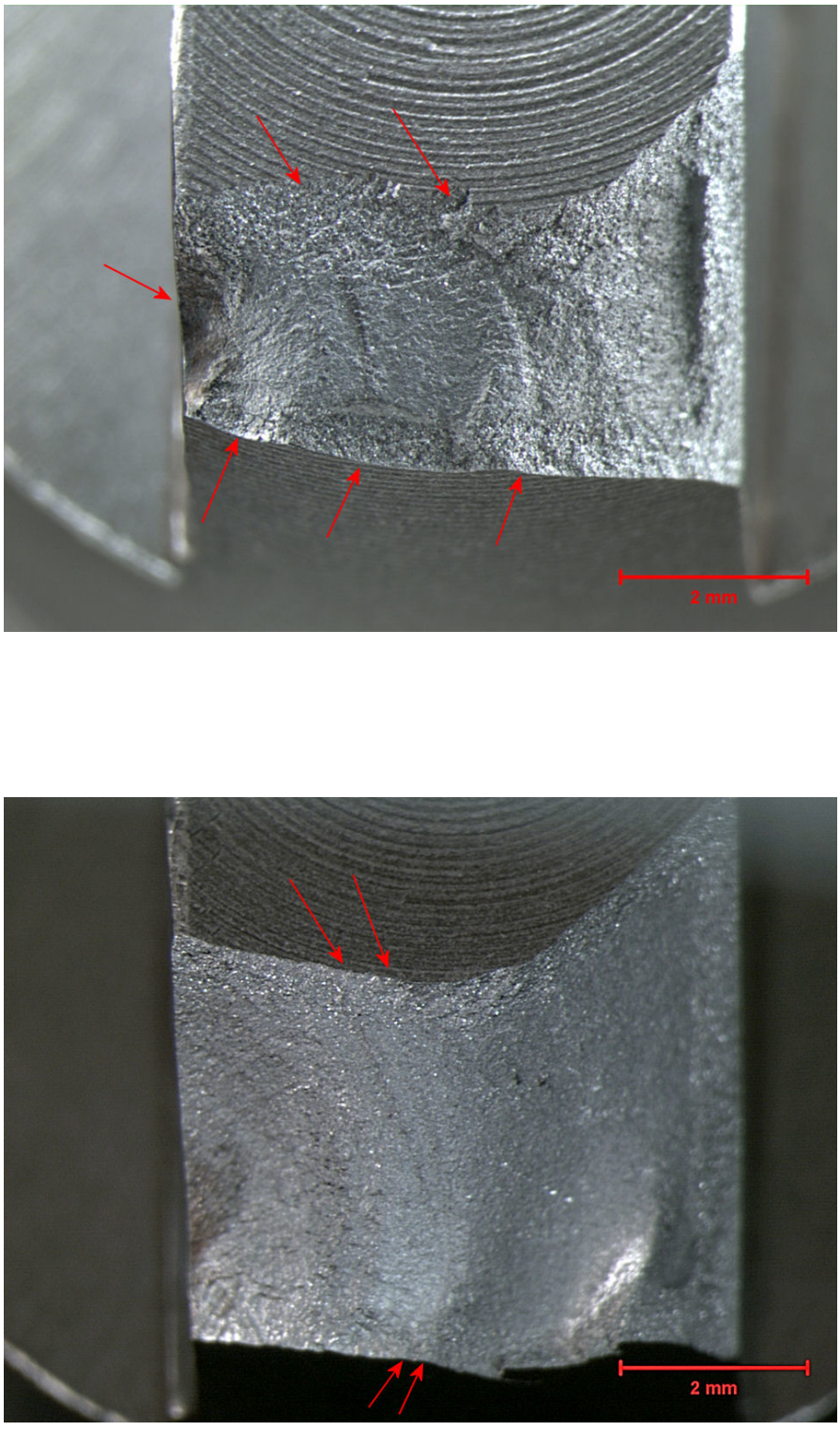

Figure 6: The surfaces of both sides of the completely fractured jack shaft showed evidence of beach marks (at arrows).

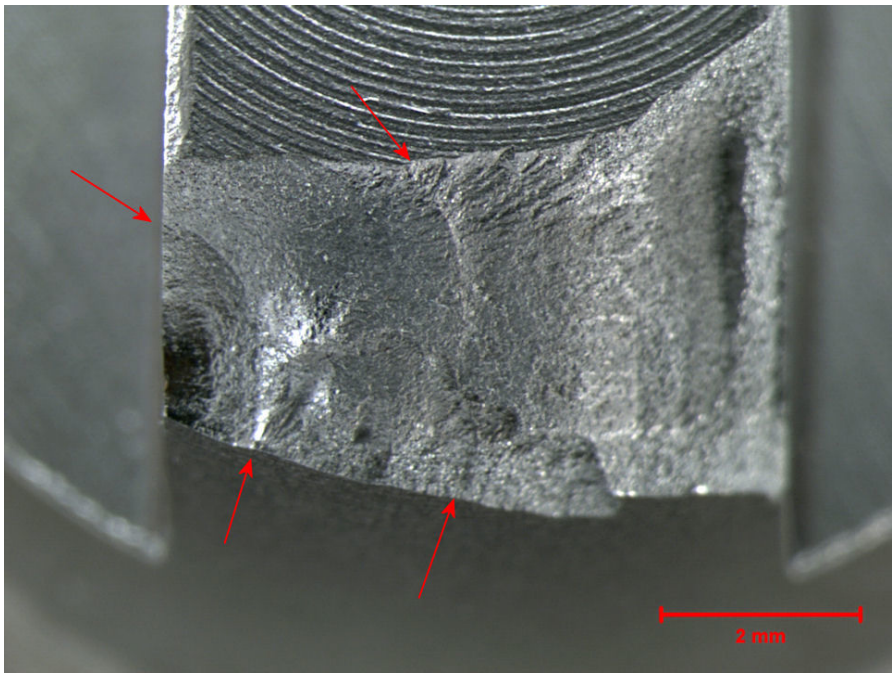

Figure 7: The exposed crack surface of the cracked jack shaft also exhibited beach marks (at arrows).

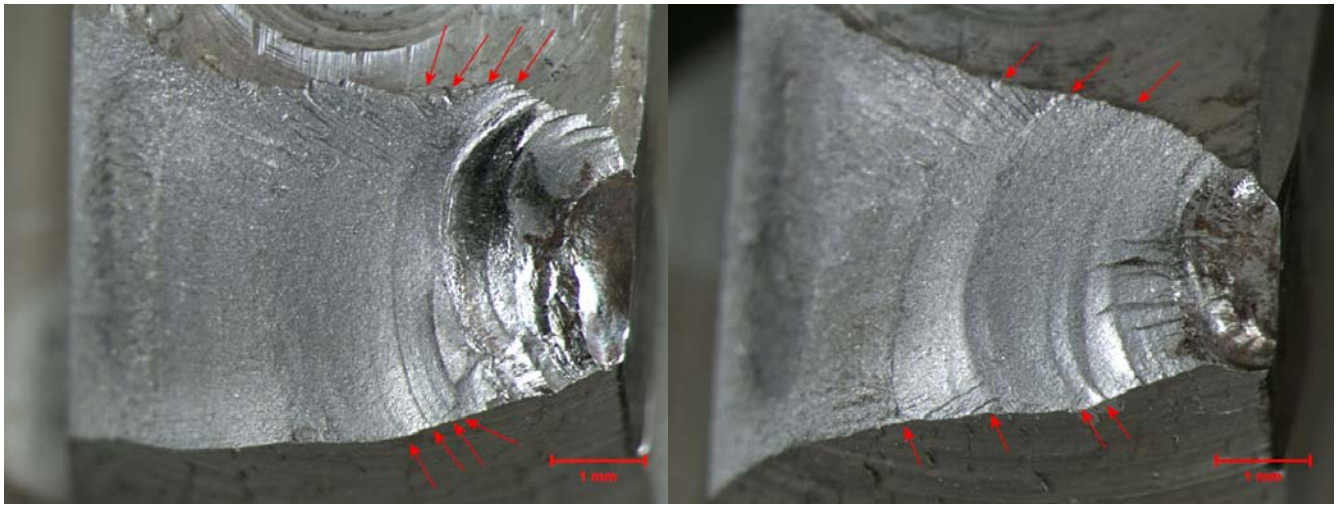

Figure 8: Fractographic features on both fracture surfaces of the 98765 shaft were similar to those observed on the jack shafts.

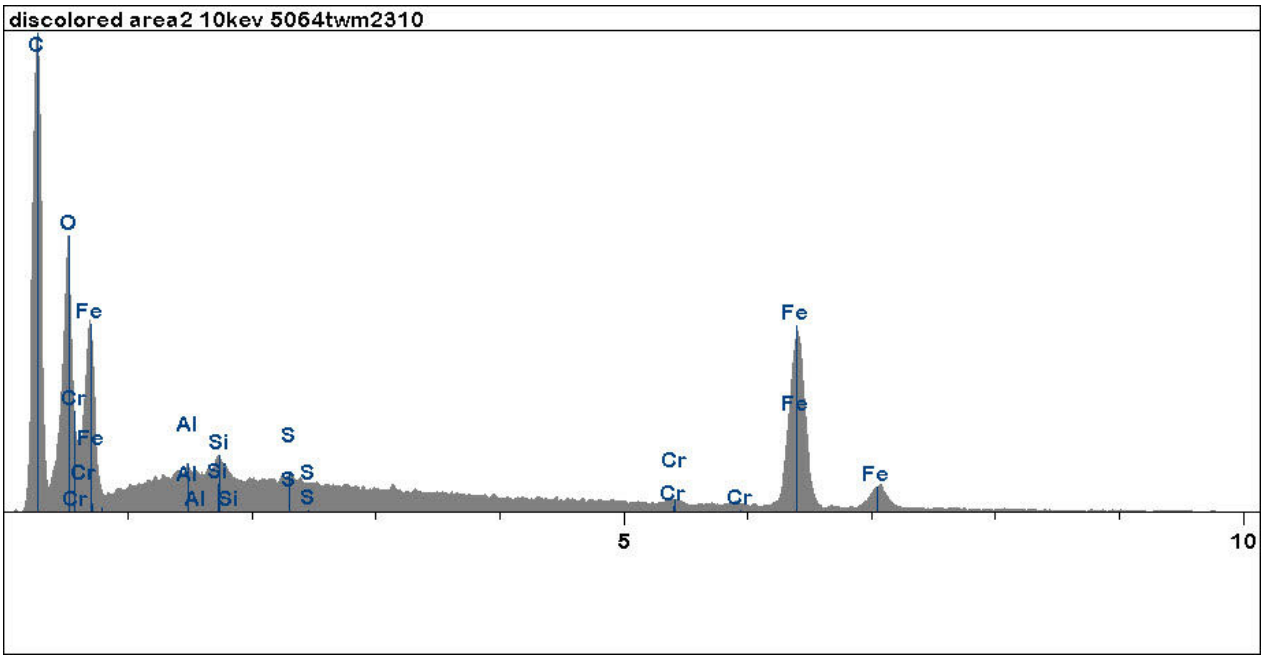

Figure 9: EDS chemical analysis of the reddish-black discoloration observed on the samples reveals carbon, oxygen and iron, with silicon, aluminum, chromium and sulfur present in lesser amounts.

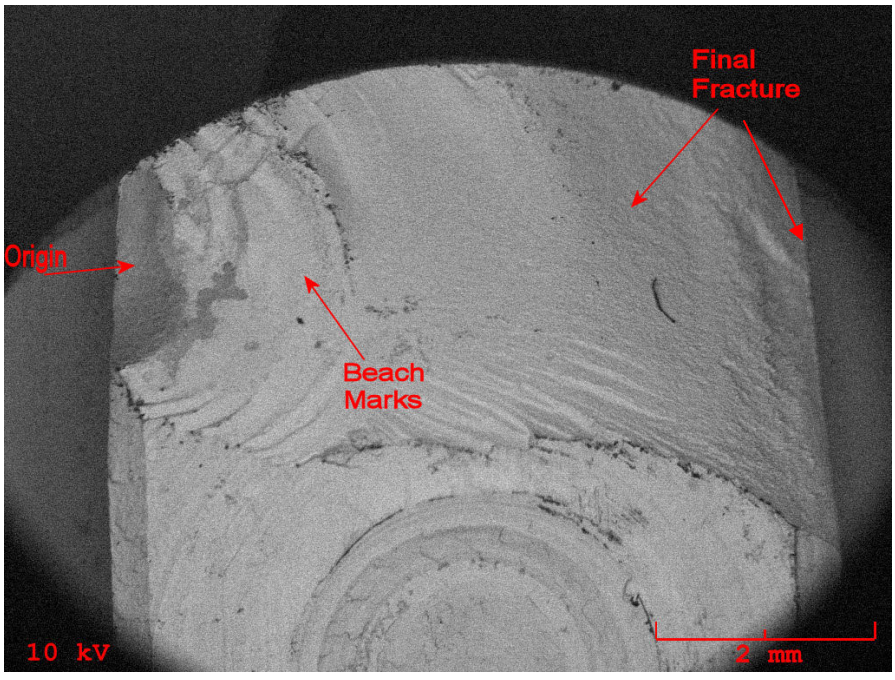

Figure 10: Low magnification backscatter electron image view of a typical fracture surface, showing the general locations of higher magnification images.

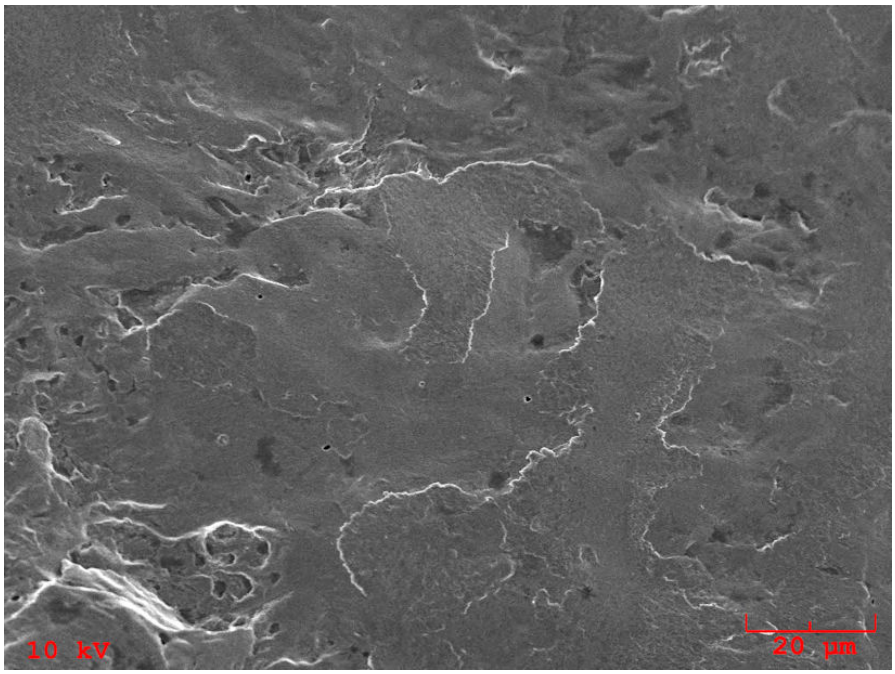

Figure 11: Secondary electron image of a jack shaft fracture near the origin. Fractographic features have been obliterated by post-fracture rubbing.

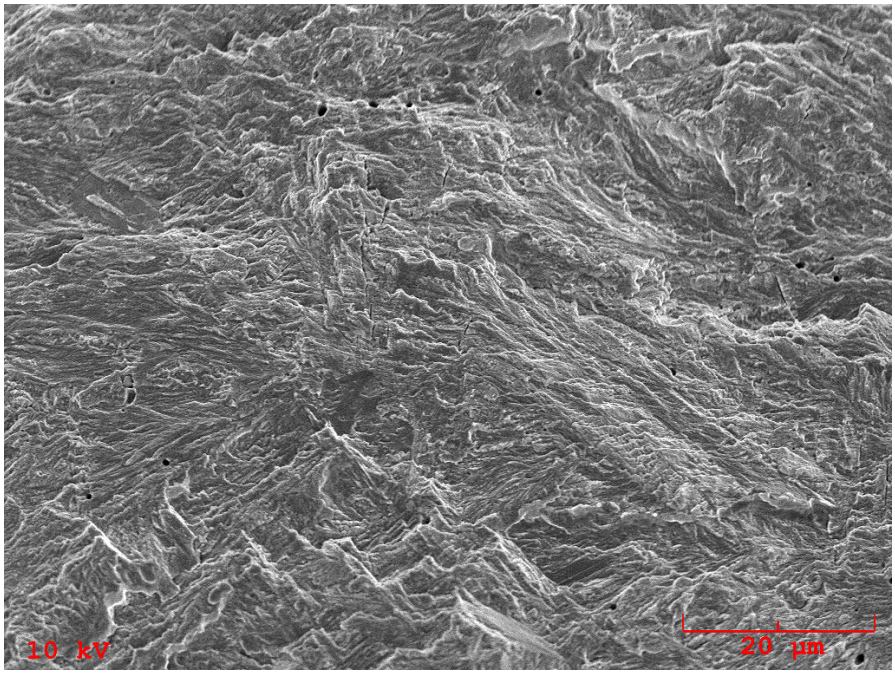

Figure 12: Secondary electron image of a jack shaft fracture from the region of visible beach marks, showing fractographic features consistent with fatigue.

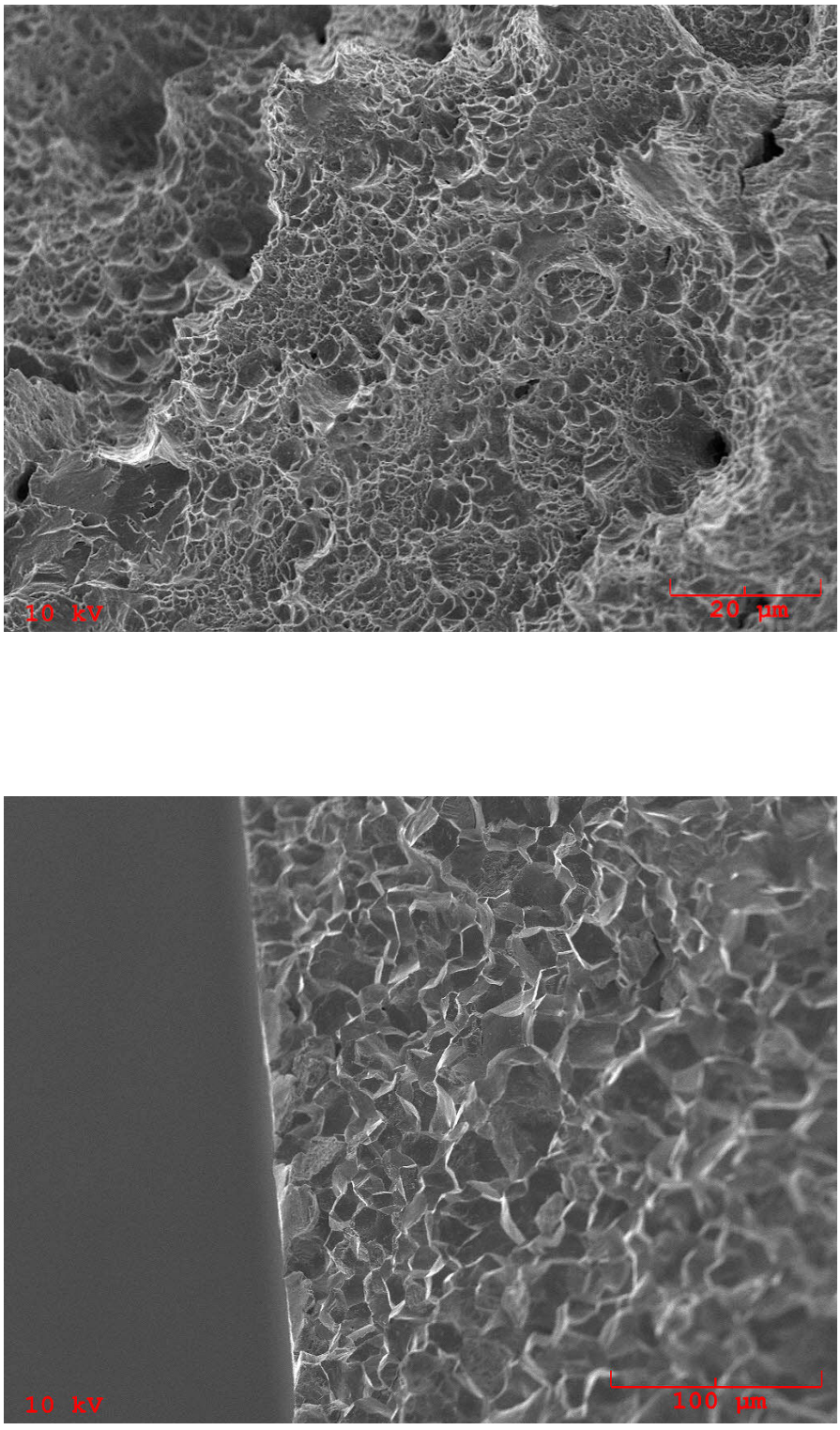

Figure 13: Final overload regions of the jack shaft fractures were comprised of dimpled rupture in the core (top image), with intergranular separation through the case-hardened area.

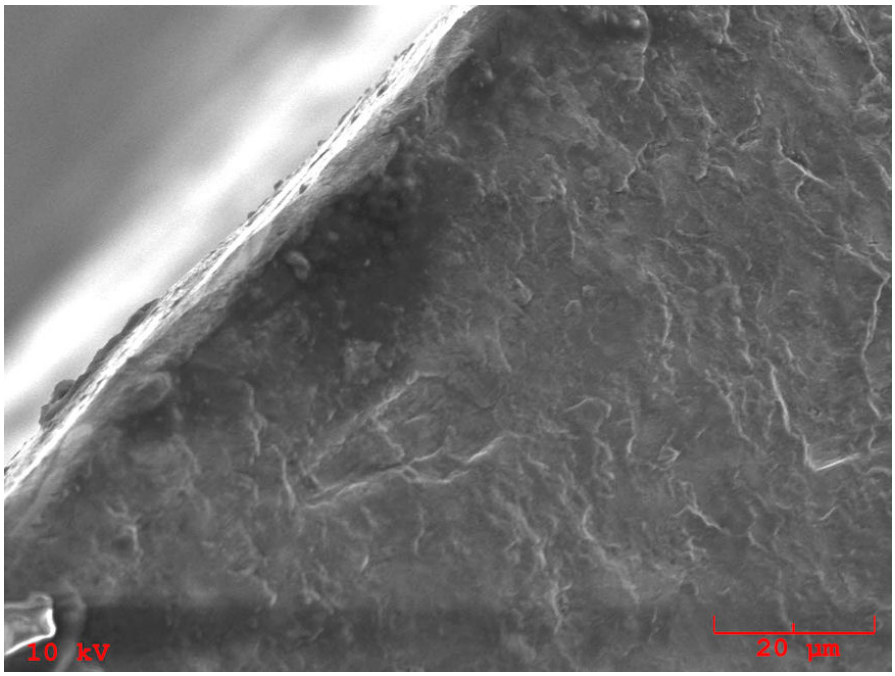

Figure 14: Secondary electron image of the 98765 shaft fracture near the origin. Fractographic features have been obliterated by post-fracture rubbing.

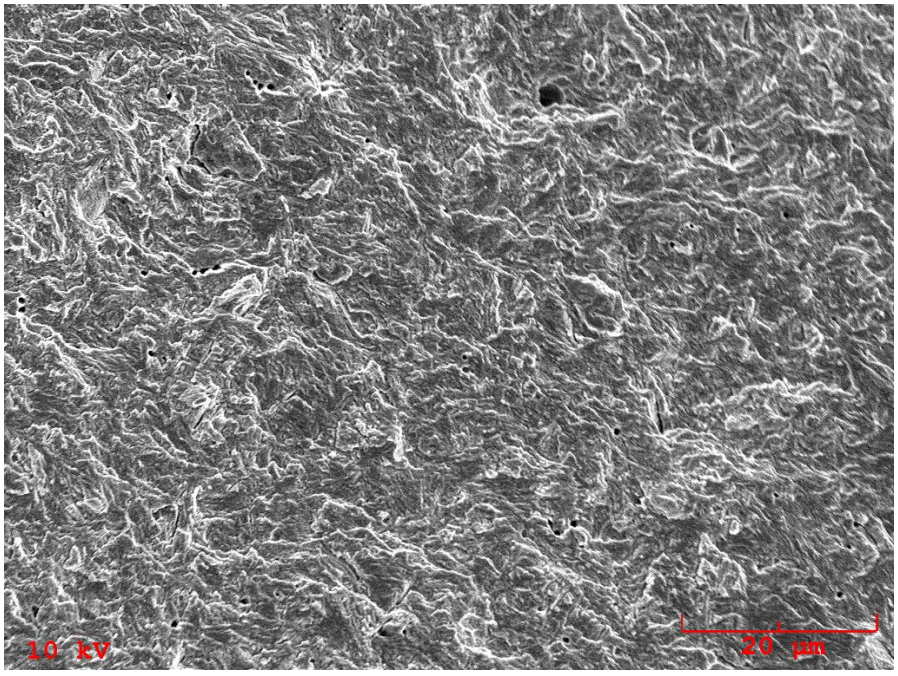

Figure 15: Secondary electron image of the 98765 shaft fracture in the region of visible beach marks, showing evidence of fatigue.

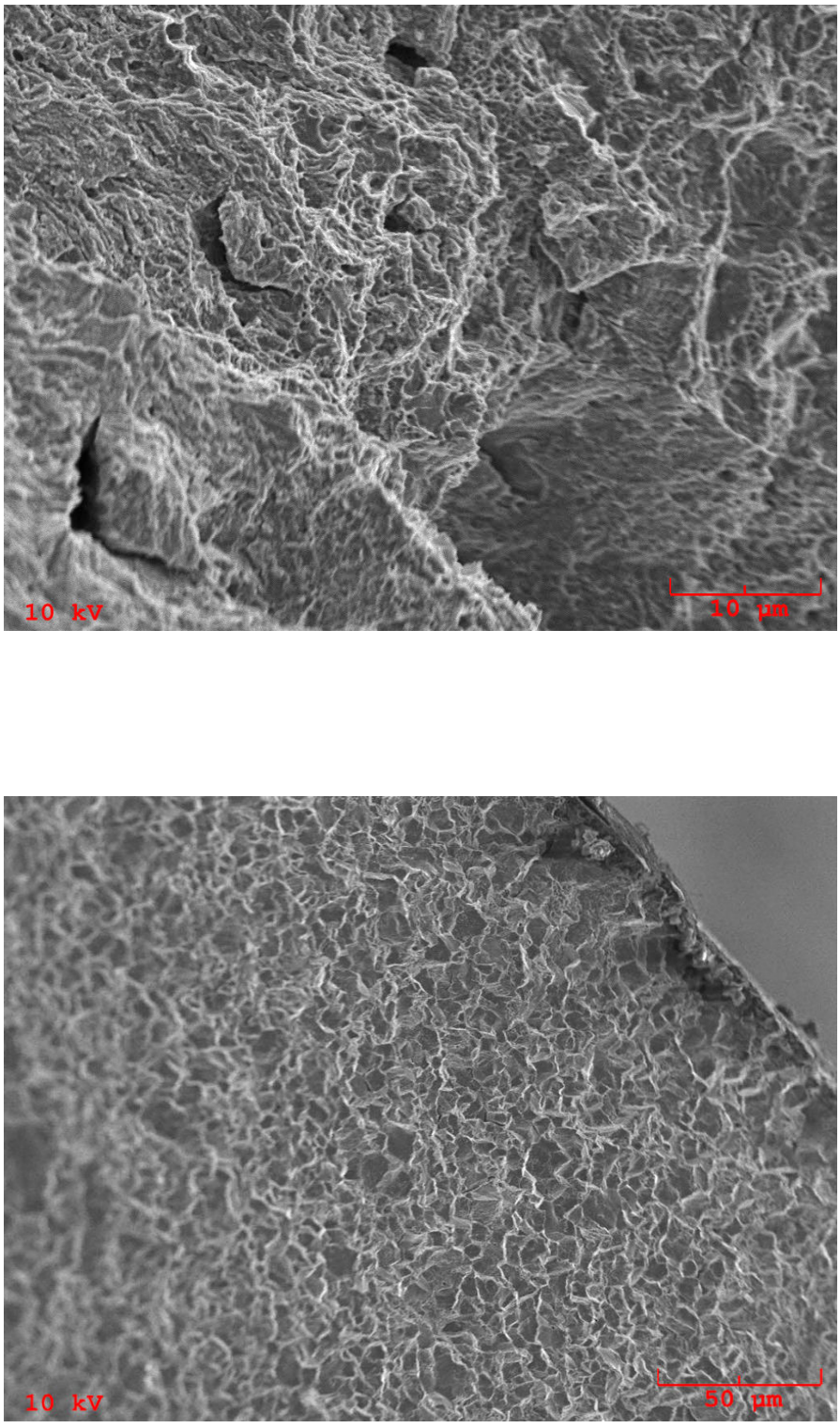

Figure 16: Final overload regions of the 98765 shaft also consisted of dimpled rupture in the core (top image), with intergranular separation through the case-hardened area.

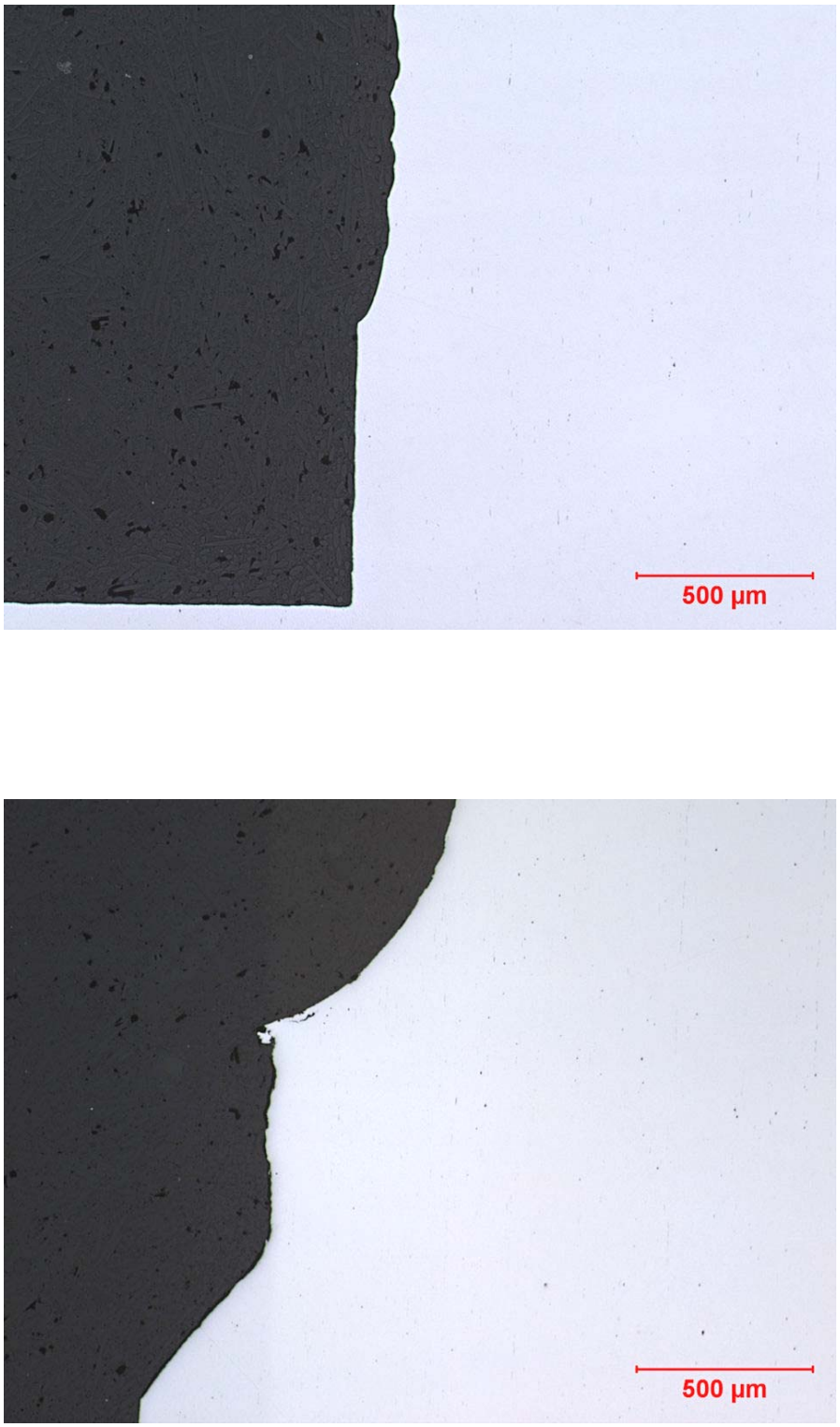

Figure 17: Images showing the material loss in the worn regions of the jack shaft (top image) and 98765 gear shaft. Material loss on the gear shaft was much more pronounced.

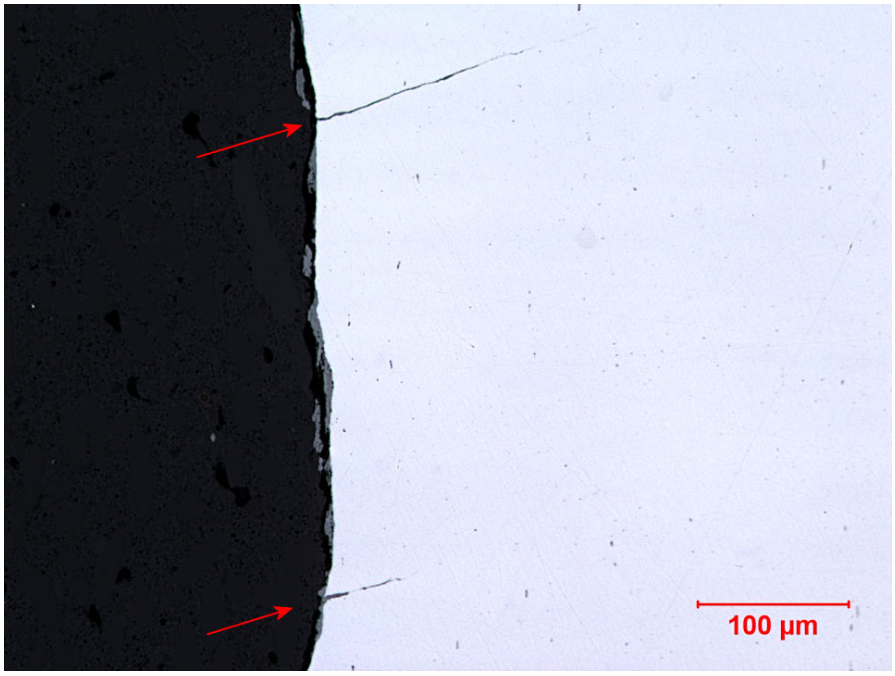

Figure 18: Secondary cracks were observed in the worn area below the main fracture on the jack shaft with fractures at both engagement regions.

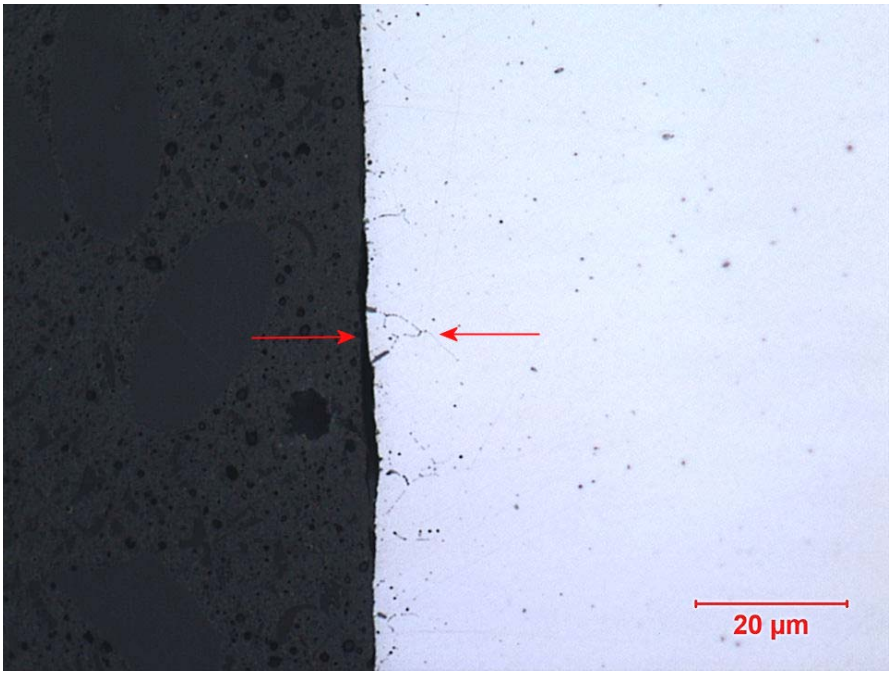

Figure 19: Intergranular oxidation (between arrows) observed in the jack shaft with the incomplete fracture.

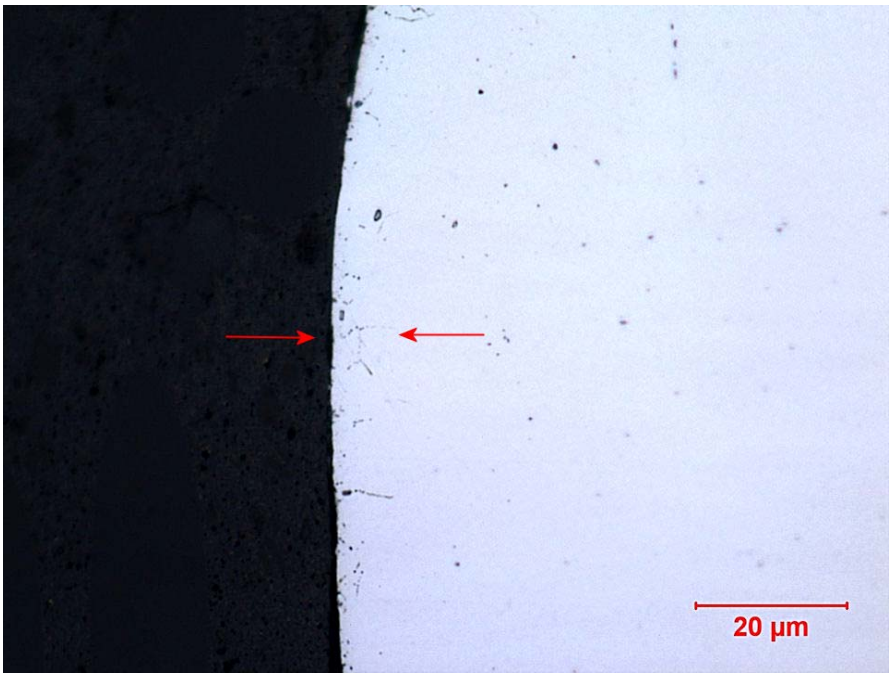

Figure 20: Intergranular oxidation (between arrows) observed in the jack shaft with fractures at both contact points.

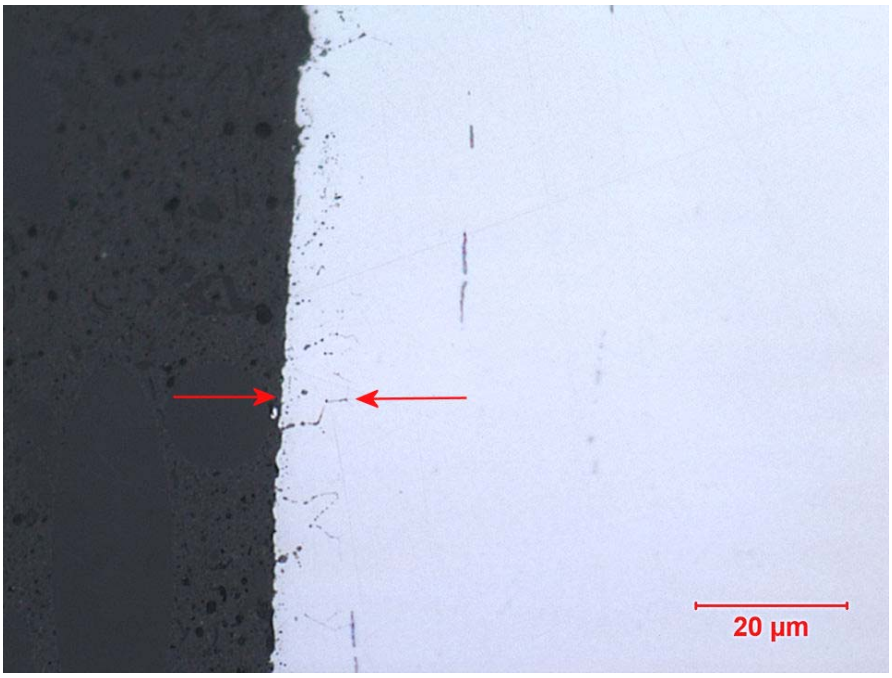

Figure 21: Intergranular oxidation (between arrows) observed in the 98765 gear shaft.

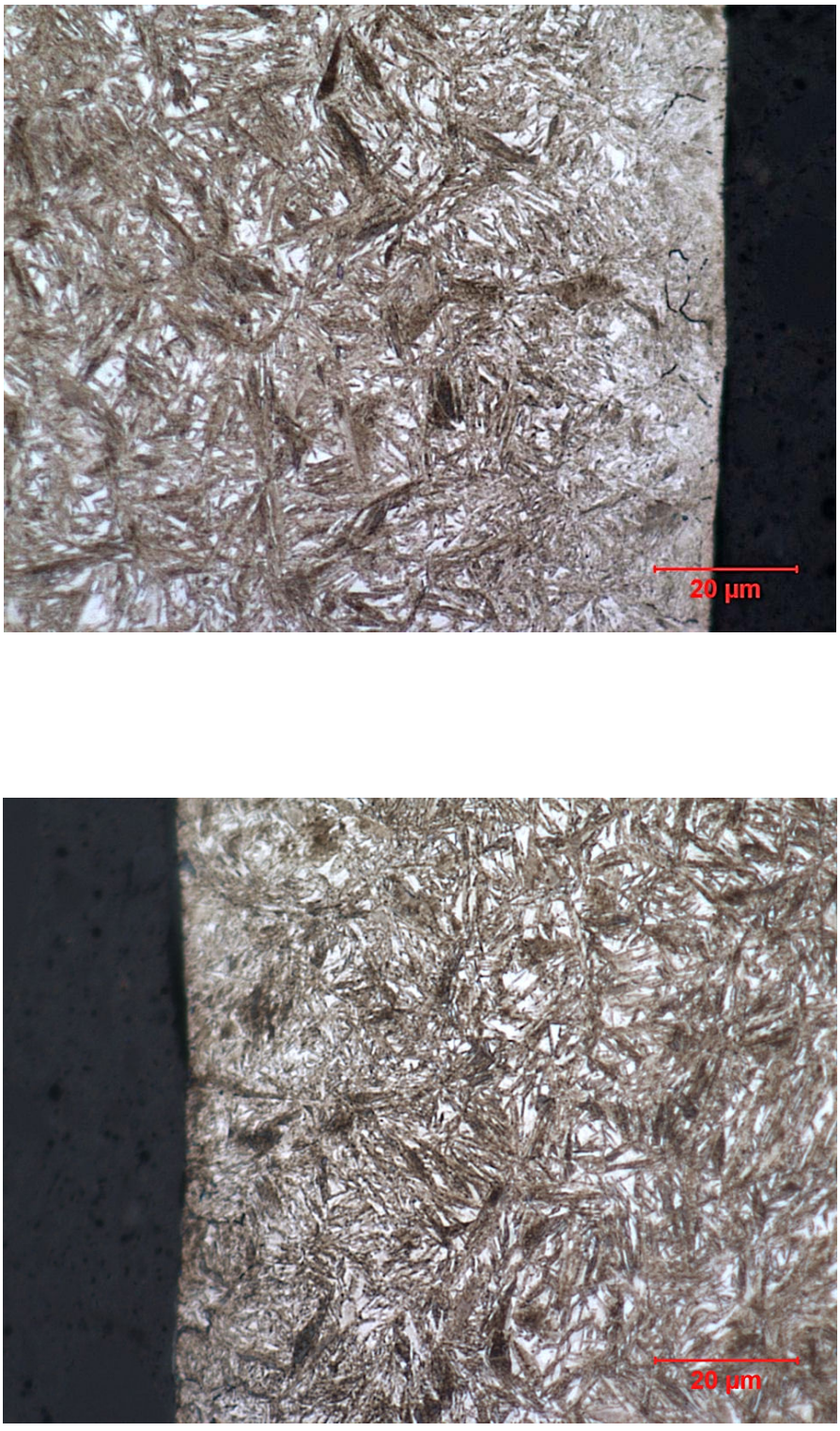

Figure 22: The case microstructure of both jack shafts (top image – jack shaft fractured at both engagement points) showed significant amounts of retained austenite (white constituent).

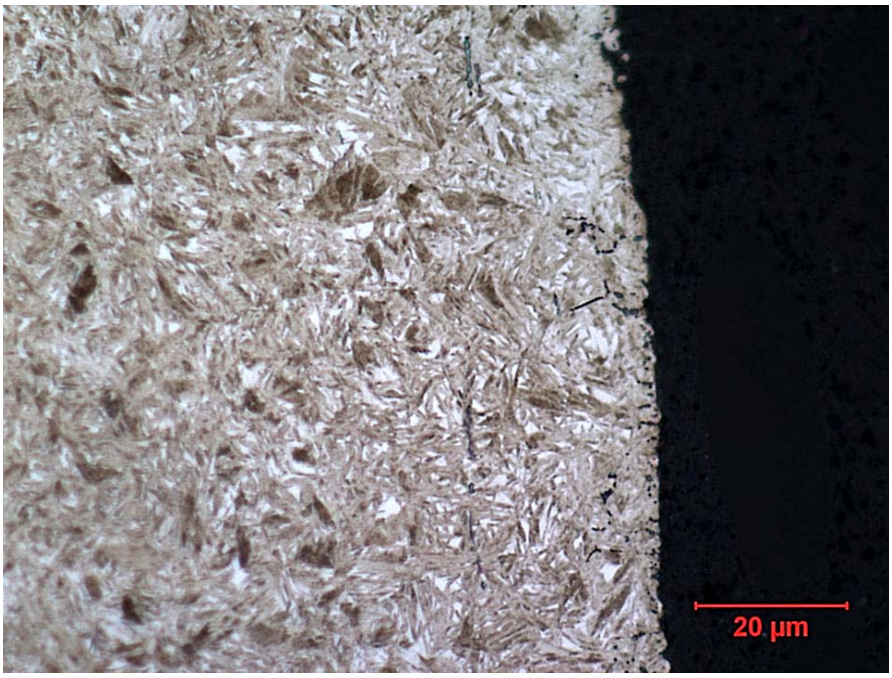

Figure 23: The 98765 gear shaft case also contained retained austenite.

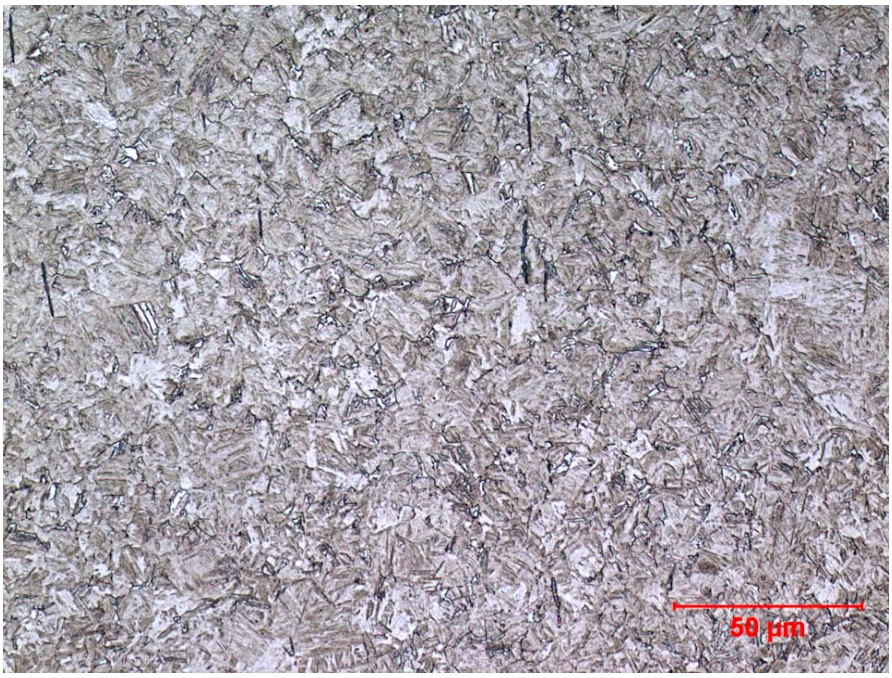

Figure 24: The core microstructure of all three fractured components was similar, consisting of martensite and small amounts of grain boundary ferrite.

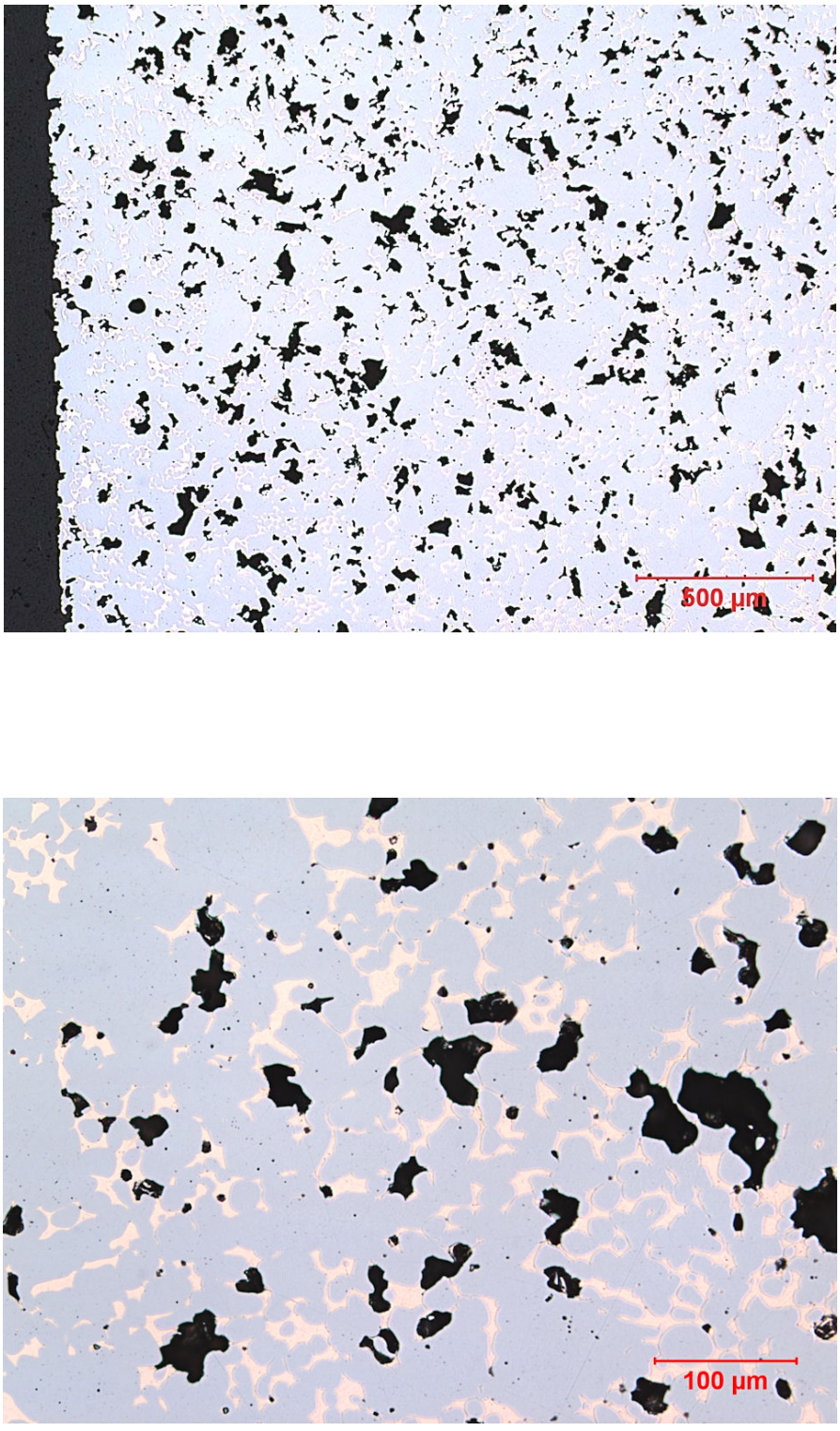

Figure 25: As polished view of the jack shaft utilized for comparison, showing typical porosity distribution and morphology. Note the presence of copper.

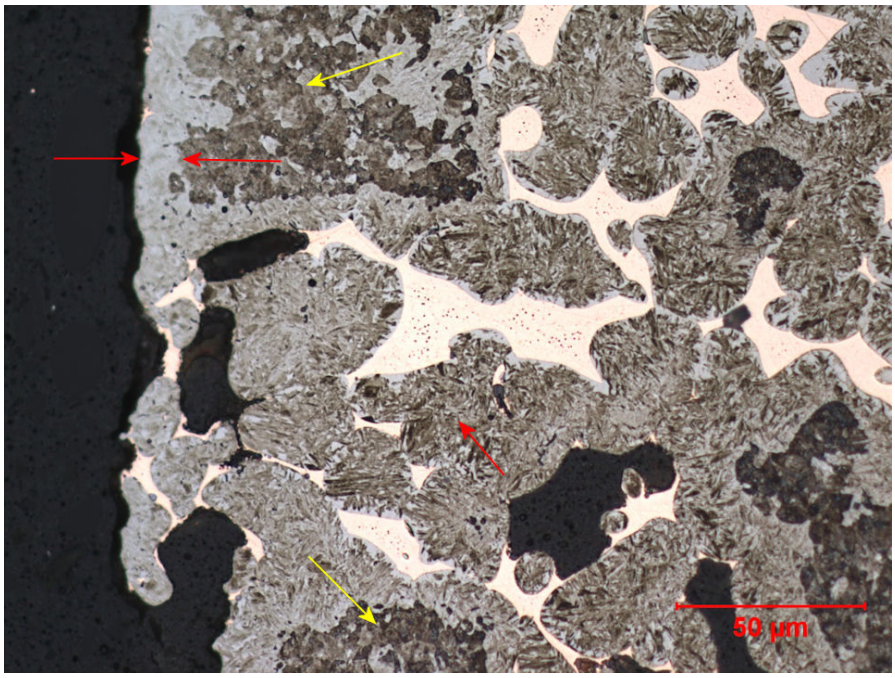

Figure 26: Microstructure of the comparison jack shaft in the contact regions was comprised of fully hardened martensitic regions (red arrows) and areas of upper transformation products (yellow arrows).

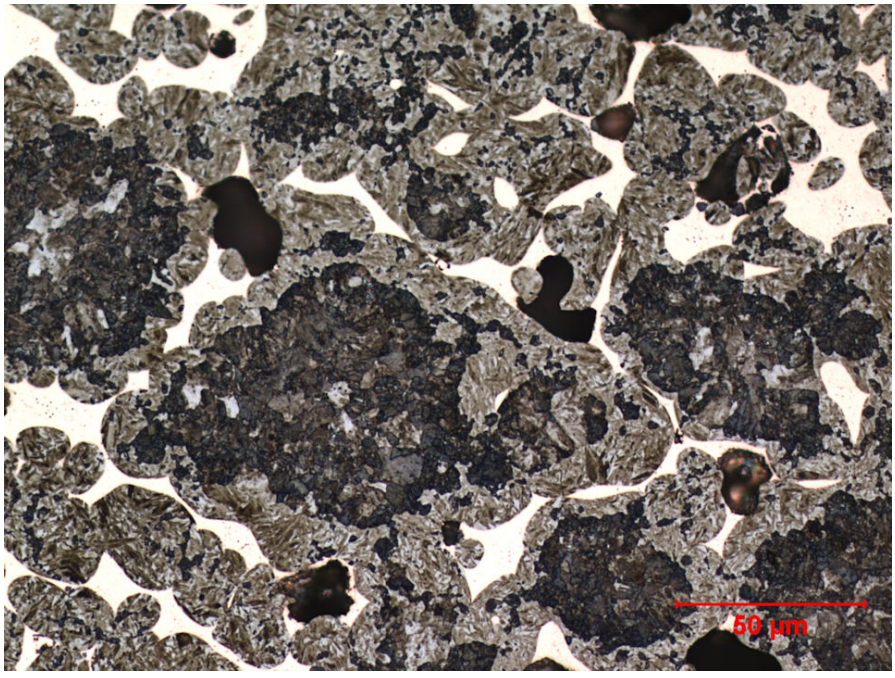

Figure 27: Core microstructure of the comparison jack shaft also consists of a mixture of martensite, bainite and fine pearlite.